J|A|C|S COMMUNICATIONS

Published on Web 12/18/2008

Dynamic Intracomplex Heterogeneity of Phytochrome

Jana B. Nieder, Marc Brecht,* and Robert Bittl

Fachbereich Physik, Freie Universität Berlin, Arnimallee 14, 14195 Berlin, Germany

Received July 25, 2008; E-mail: marc.brecht@physik.fu-berlin.de

Phytochromes are photoreceptors in plants, bacteria, and fungi.[1] They control a variety of light-regulated processes, e.g., germination, photomorphogenesis, and flowering of plants.[2] The phytochrome function is based on the interplay of two protein parts, a sensing (receptor) module, and a signaling module (kinase). The photoactive module reacts on light with conformational changes of its covalently bound open chain tetrapyrrole chromophore.[3−5] The dark stable state is in most phytochromes the red-light absorbing P_R state ($\lambda_{max} \approx 550-700$ nm). Within ∼5−100 ps after photoactivation an isomerization of the chromophore occurs.[6] The nonfluorescent photoproduct P_{FR} absorbs far red light ($\lambda_{max} \approx 600-750$ nm) as seen in UV−vis spectra taken before and after photoactivation.[7] The isomerization is photoreversible, and P_{FR} also undergoes thermally activated dark reversion to P_R.[8] The conformational changes of the chromophore during the photocycle cause rearrangements of the surrounding protein,[9,10] leading to signal transduction.

Recently, structural models for the chromophore binding domain in the P_R state became available[11,12] which are considered representative for the phytochrome superfamily. The structures reveal that phytochromes enclose bulk water around their chromophore via hydrogen bonds building up a so-called pyrrol−water network. Phytochromes have extensively been analyzed by various spectroscopic methods as flash photolysis,[13] Fourier Transform Infra-Red (FT-IR),[14] and Resonance Raman (RR)[15,16] spectroscopy. Interestingly, the obtained results are marked by a high degree of variance. A comprehensive phytochrome review therefore was entitled "Photophysics and photobiochemistry of the heterogeneous phytochrome system".[17] Ground-state as well as excited-state heterogeneity has been discussed.[18] Multicomponent kinetics observed by fluorescence decay analysis[19] and recently by ultrafast spectroscopic techniques[20] are examples for functional heterogeneity, and new RR data on solution and single-crystal samples[21] are interpreted in terms of structural heterogeneity of the chromophore. An assignment of spectroscopically derived parameters and disentangling heterogeneous subgroups is difficult or even impossible in ensemble spectroscopy, especially when dealing with complex vibrational data. Therefore, we go beyond ensemble-averaged spectroscopy to directly investigate the presumed phytochrome heterogeneity on the single-molecule level and study the fluorescent ground-state P_R by means of single-molecule fluorescence emission spectroscopy.

Protein expression, extraction, and purification of the phytochrome Agp1 from *Agrobacterium tumefaciens* are described elsewhere.[8] Agp1 solutions were highly diluted to concentrations of 10^{-9} to 10^{-10} M in a 30% w/w glycerol/Tris-HCl buffer (50 mM Tris, 5 mM EDTA, 150 mM NaCl with pH 7.8); this concentration yields Agp1 monomers (dimer dissociation constant is 5 ± 3 μM for Cph1 from *Synechocystis*[22]) and conditions suitable for single-molecule detection. The experimental setup was a home-built confocal spectrometer designed for measurements at cryogenic temperatures ($T = 1.4$ K) described recently.[23] For experiments on Agp1, the excitation source and filter set were adapted. A $\lambda = 680$ nm diode laser (Schäfter-Kirchhoff, 57FCM) attenuated to 100−600 μW, a cleanup filter with transmission within 680 ± 5 nm, and a long pass filter with $\lambda_T > 695$ nm (AHF Analysentechnik) were used. The vibronic excitation at $\lambda_{exc} = 680$ nm below the absorption maximum of P_R in Agp1 ($\lambda_{max} \approx 700$ nm) is advantageous in low temperature single-molecule fluorescence spectroscopy.[24] The samples were dark adapted prior to freezing to the measurement temperature $T = 1.4$ K. At this temperature all transitions within the photocycle of phytochrome are frozen out;[25] thus we observe exclusively the P_R state.

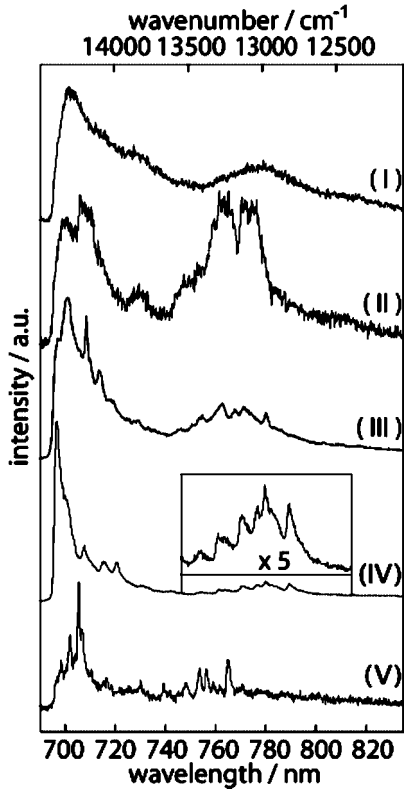

Figure 1. Representative single-molecule fluorescence spectra of individual Agp1 phytochromes ($\lambda_{exc} = 680$ nm, $t_{acq} = 40$ s, $T = 1.4$ K).

Low temperature fluorescence emission spectra were taken from 80 individual phytochrome complexes. A selection of representative spectra with an acquisition time $t_{acq} = 40$ s is depicted in Figure 1. They visualize the observed continuous transition from broad fluorescence bands to narrow emission lines dependent on the individual molecule. Most spectra show fluorescence intensity within two broad wavelength intervals, one centered at ∼710 nm and the second at ∼770 nm. Interestingly, the energy difference between these two prominent bands lies within the vibrational fingerprint region of the phytochrome chromophore (∼1100−1700 cm^{-1}), where C=C

10.1021/ja8058292 CCC: $40.75

stretching and N—H bending modes are observed in FT-IR[14] and RR[21] spectroscopy.

Large differences occur for the line width, band, and intensity distributions as well as exact peak positions. The line width of the emission lines shows a variance of more than 1 order of magnitude, ranging from $\Gamma_{fwhm} \approx 30$ nm (≈ 500 cm^{-1}; spectrum I) to $\Gamma_{fwhm} \approx 1$ nm (≈ 15 cm^{-1}; spectrum V) close to the spectral resolution limit of our setup. While spectrum I shows broad emission bands, spectrum II is marked by a double peak structure in both emission bands and additionally shows contributions at 730 and 750 nm. Spectrum III shows similar broad emission bands as spectrum I, but additional narrow line features (~5 nm) lie on top of these broad fluorescence contributions. These additional lines have very similar line widths and unequal distances between each other. In spectrum IV the relative intensity between the broad band at 770 nm and the superimposed narrow lines is strongly shifted toward the narrow lines (see inset at IV). In spectrum V even narrower lines (~1 nm) are detected but with the longer wavelength spectral center shifted toward 760 nm. The partially resolved lines in the 740 to 780 nm region, with a distance of ~1100−1700 cm^{-1} from the emission maxima, are similar to narrow fluorescence line structures detected from conjugated polymers[26−28] and dendrimeric structures,[29,30] which were assigned to vibrational modes.

Further heterogeneity is observed in the intensity distribution. Whereas mostly the shorter wavelength contribution clearly dominates, exceptions are observed, e.g., in spectrum II. The observation of drastically different emission spectra confirms on the single-molecule level the idea of a strong heterogeneity of phytochrome. To gain a deeper insight into the characteristics of the fluorescence fingerprints of single phytochrome molecules their time dependence on the second time scale was observed.

Figure 2a shows a series of spectra from an individual Agp1 phytochrome molecule. These spectra were collected with the minimum acquisition time $t_{acq} = 0.2$ s providing a sufficient signal-to-noise ratio for Agp1 in our setup. The fluorescence intensity is color-coded. At the beginning of the observation the two dominant fluorescence lines show a rather stable emission wavelength. After a transition to a dark state, the fluorescence reappears. However, the emission wavelength now undergoes changes in the range of a few nanometers with a rate similar to the time resolution of the experiment. This jump rate on the sub-second time scale and the jump width of the order of 100 cm^{-1} are comparable to those of a dye in an amorphous polymer matrix.[24]

In the third interval, again after a transition to a dark state, the spectral changes are accelerated further, such that the underlying spectral lines cannot be observed individually anymore. In Figure 2b the spectra averaged over 2 s within these three different emission periods are presented. They show that an individual phytochrome molecule undergoes dynamic changes between states characterized by the different fluorescence emission properties seen in Figure 1, namely from type V in period (i) to type IV in period (ii) and then to the broadened type I in period (iii). Thus, fluorescence single-molecule spectroscopy not only confirms intercomplex heterogeneity but also shows a dynamic intracomplex heterogeneity of phytochromes.

Another example of strong time-dependent intracomplex heterogeneity is shown in Figure 3a. The sequence of spectra has a time resolution of 1 s. Instead of observing stable fluorescence fingerprints, again strong spectral dynamics occur. Selected spectra from the time-dependent series are depicted in Figure 3b. Here the spectral changes, often designated spectral diffusion, occur rather frequently. Therefore, intense narrow sharp lines, similar to the fluorescence signal in spectrum 44, are rarely detected. Mainly

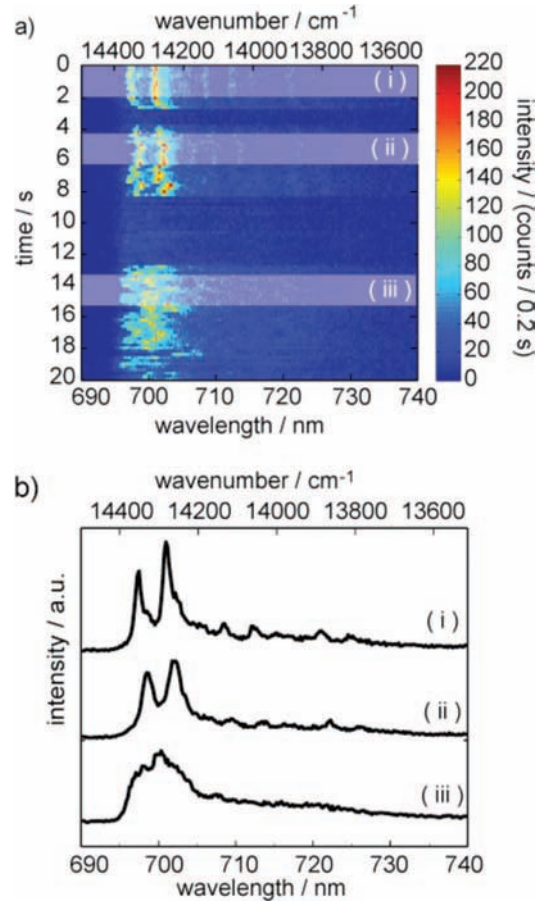

Figure 2. (a) 2D representation of a series of time-dependent spectra taken from one single phytochrome molecule ($\lambda_{exc} = 680$ nm, $t_{acq} = 0.2$ s per spectrum, $T = 1.4$ K). (b) spectra obtained by averaging over the highlighted 2 s intervals in (a).

multiple lines like those in spectrum 58 are observed, where several changes of the emission wavelength occurred within the acquisition period. Broadened features like those in spectrum 9 are observed if the spectral diffusion rate is even higher. As a consequence, the observed line width increases with increasing accumulation times. This is exemplified in Figure 3c. Thus, the time-dependent spectrally resolved single-molecule data show spectral diffusion as the origin of line broadening and the similarity of time-averaged single-molecule spectra of type I with ensemble fluorescence spectra.

Phytochromes are natural one-chromophore binding molecules. They are an excellent choice for the analysis of interactions between a pigment and its protein surrounding. The static single-molecule fluorescence spectra revealed different spectral types with a high diversity of emission fingerprints from the P_R state. Most striking is the variation in the observed line widths, differing by more than 1 order of magnitude. This observation corroborates the ensemble data from various spectroscopic techniques concerning the heterogeneity of phytochromes.

Moreover, time-resolved single-molecule spectroscopy showed that this heterogeneity is observable within one single phytochrome molecule as a time-dependent phenomenon even at very low temperatures. The dynamic changes lead to different spectral forms varying in their line widths, fluorescence peak positions, and intensity distributions. Thereby, these time-dependent measurements revealed the source of line broadening in time-averaged spectra. The characteristics of spectral diffusion are not statically associated with the individual molecules but also vary in time for each molecule.

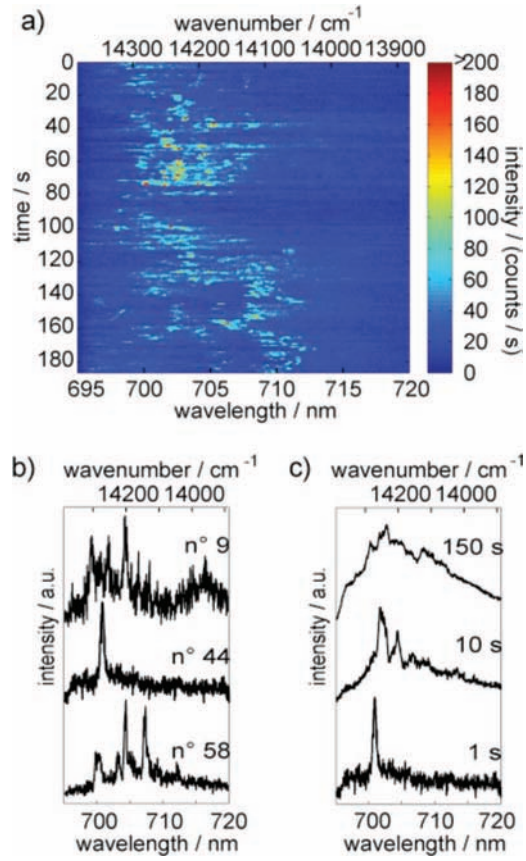

Figure 3. (a) 2D representation of a series of time-dependent spectra (λ_{exc} = 680 nm, t_{acq} = 1 s per spectrum, T = 1.4 K). (b) Selected 1 s spectra from the series and (c) spectra averaged over different indicated time intervals.

Under the employed low temperature conditions, where conformational changes are largely frozen out, only minor conformational alterations have to be taken into account to explain the spectral dynamics. The switching of phytochromes between the different spectral forms at these extremely low temperatures requires rather low barriers between the conformational states or tunneling processes as a source of the different emission properties. The pyrrole−water network in the direct chromophore environment is a likely candidate for a structure with such shallow potential energy minima or for tunneling processes since hydrogen movement remains possible at 1.4 K.[31] Significant shifts in the emission wavelength might be induced by small-scale proton movements along the deprotonation/reprotonation coordinate followed later in the photocycle.[13] A direct comparison of the dynamic processes observed here at low temperatures on the second time scale with conformational exchange monitored on the micro- to millisecond time scale in NMR experiments[32] at ambient temperatures is impossible at present.

Broadened spectral shapes are observed in the limit of fast spectral diffusion compared to the experimental time resolution. In this case, the intrinsic line shape is no longer detectable. The occurrence of this fast spectral diffusion is a likely reason for the lack of results from site-selective ensemble techniques, e.g., spectral hole-burning, on phytochrome.

During periods of slow spectral diffusion with respect to the time resolution of the setup, the underlying spectral information of the pigment in its natural protein environment becomes accessible. In this case highly resolved spectra with a multitude of narrow lines were detected. Their distances from the main emission are compatible with an assignment to vibrational modes. Vibrational data from an individual pigment in its natural protein environment have, to our knowledge, not been reported before.

Acknowledgment. We thank Prof. Tilman Lamparter (Universität Karlsruhe) for the Agp1 samples and acknowledge support from the Cluster of Excellence "Unifying Concepts in Catalysis" funded by the Deutsche Forschungsgemeinschaft.

References

(1) Quail, P. H. *Nat. Rev. Mol. Cell Biol.* **2002**, *3*, 85–93.
(2) Rockwell, N. C.; Su, Y. S.; Lagarias, J. C. *Annu. Rev. Plant Biol.* **2006**, *57*, 837–858.
(3) Rüdiger, W.; Thümmler, F. *Angew. Chem., Int. Ed. Engl.* **1991**, *30*, 1216–1228.
(4) Andel, F.; Hasson, K. C.; Gai, F. *Biospec.* **1997**, *3*, 421–433.
(5) Borucki, B. *Photochem. Photobiol. Sci.* **2006**, *5*, 553–566.
(6) Heyne, K.; Herbst, J.; Stehlik, D.; Esteban, B.; Lamparter, T.; Hughes, J.; Diller, R. *Biophys. J.* **2002**, *82*, 1004–1016.
(7) Lamparter, T.; Carrascal, M.; Michael, N.; Martinez, E.; Rottwinkel, G.; Abian, J. *Biochemistry* **2004**, *43*, 3659–3669.
(8) Lamparter, T.; Michael, N.; Mittmann, F.; Esteban, B. *Proc. Natl. Acad. Sci. U.S.A.* **2002**, *99*, 11628–11633.
(9) Noack, S.; Michael, N.; Rosen, R.; Lamparter, T. *Biochemistry* **2007**, *46*, 4164–4176.
(10) Park, C.-M.; Bhoo, S.-H.; Song, P.-S. *Semin. Cell Dev. Biol.* **2000**, *11*, 449–456.
(11) Wagner, J. R.; Brunzelle, J. S.; Forest, K. T.; Vierstra, R. D. *Nature* **2005**, *438*, 325–331.
(12) Yang, X.; Stojkovic, E.; Kuk, J.; Moffat, K. *Proc. Natl. Acad. Sci. U.S.A.* **2007**, *104*, 12571–12576.
(13) Borucki, B.; von Stetten, D.; Seibeck, S.; Lamparter, T.; Michael, N.; Mroginski, M. A.; Otto, H.; Murgida, D. H.; Heyn, M. P.; Hildebrandt, P. *J. Biol. Chem.* **2005**, *280*, 34358–34364.
(14) Foerstendorf, H.; Benda, C.; Gärtner, W.; Storf, M.; Scheer, H.; Siebert, F. *Biochemistry* **2001**, *40* (49), 14952–14959.
(15) Andel, F.; Murphy, J. T.; Haas, J. A.; McDowell, M. T.; van der Hoef, I.; Lugtenburg, J.; Lagarias, J. C.; Mathies, R. A. *Biochemistry* **2000**, *39*, 2667–2676.
(16) Mroginski, M. A.; Murgida, D. H.; von Stetten, D.; Kneip, C.; Mark, F.; Hildebrandt, P. *J. Am. Chem. Soc.* **2004**, *126*, 16734–16735.
(17) Sineshchekov, V. A. *Biochim. Biophys. Acta* **1995**, *1228*, 125–164.
(18) van Thor, J. J.; Ronayne, K. L.; Towrie, M. *J. Am. Chem. Soc.* **2007**, *291*, 126–132.
(19) Holzwarth, A.-R.; Venuti, E.; Braslavsky, S. E.; Schaffner, K. *Biochim. Biophys. Acta* **1992**, *1140*, 59–68.
(20) Schumann, C.; Gross, R.; Michael, N.; Lamparter, T.; Diller, R. *Phys. Chem. Chem. Phys.* **2007**, *8*, 1657–1663.
(21) von Stetten, D.; Günther, M.; Scheerer, P.; Murgida, D. H.; Mroginski, M. A.; Krauss, N.; Lamparter, T.; Zhang, J.; Anstrom, D. M.; Vierstra, R. V.; Forest, K. T.; Hildebrandt, P. *Angew. Chem., Int. Ed.* **2008**, *47*, 4753–4755.
(22) Otto, H.; Lamparter, T.; Borucki, B.; Hughes, J.; Heyn, M. P. *Biochemistry* **2003**, *42*, 5885–5895.
(23) Brecht, M.; Studier, H.; Elli, A. F.; Jelezko, F.; Bittl, R. *Biochemistry* **2007**, *46*, 799–806.
(24) Kiraz, A.; Ehrl, M.; Bräuchle, C.; Zumbusch, A. *J. Chem. Phys.* **2005**, *123*, 10821–10824.
(25) Andel, F.; Lagarias, J. C.; Mathies, R. A. *Biochemistry* **1996**, *35*, 15997–16008.
(26) Heun, S.; Mahrt, R. F.; Greiner, A.; Lemmer, U.; Bässler, H.; Halliday, D. A.; Bradley, D. D. C.; Burn, P. L.; Holmes, A. B. *J. Phys.: Condens. Matter* **1993**, *5*, 247–260.
(27) Lippitz, M.; Hubner, C. G.; Christ, T. *Phys. Rev. Lett.* **2004**, *92*, 103001.
(28) Schindler, F.; Lupton, J. M.; Feldmann, J.; Scherf, U. *Proc. Natl. Acad. Sci. U.S.A.* **2004**, *101*, 14695–14700.
(29) Métivier, R.; Christ, T.; Kulzer, F.; Weil, T.; Müllen, K.; Basché, T. *J. Lumin.* **2004**, *110*, 217–224.
(30) Feist, F. A.; Tommaseo, G.; Basché, T. *Phys. Rev. Lett.* **2007**, *98*, 208301.
(31) Brecht, M.; Studier, H.; Radics, V.; Nieder, J. B.; Bittl, R. *J. Am. Chem. Soc.,* in press.
(32) van Thor, J. J.; Mackeen, M.; Kuprov, I.; Dwek, R. A.; Wormald, M. R. *Biophys. J.* **2006**, *91*, 1811–1822.

JA8058292